J Electroceram (2012) 28:275–280
DOI 10.1007/s10832-012-9730-7

Low-temperature sintering of Li_2O-doped $BaTiO_3$ lead-free piezoelectric ceramics

Nan Ma · Bo-Ping Zhang · Wei-Gang Yang

Received: 24 November 2011 / Accepted: 16 April 2012 / Published online: 3 May 2012

Abstract Low-temperature sintering of $BaTiO_3$ ceramics using Li_2O as sintering aids was investigated with a special influences of Li_2O content (0–4 mol%) and sintering temperature (1000–1100°C) on crystalline structure and electrical properties. The sinterability of $BaTiO_3$ ceramics significantly improved by adding Li_2O, whose densification sintering temperature reduced from 1300°C to 1000°C. XRD pattern indicated that $BaTiO_3$-$x$$Li_2O$ samples were single phase with a tetragonal symmetry as x=0–0.3 mol%, while the samples became an orthorhombic symmetry as x= 0.5–4 mol%. The densification sintering temperature in which samples showed relative density higher than 90 % decreased with increasing Li_2O content. A maximum d_{33} value (200 pC/N) was obtained for the $BaTiO_3$-0.5 mol%Li_2O sample sintered at 1050°C, which is attributed to a vicinity of the phase transition and the high density. Adding Li_2O not only reduced the sintering temperature but also obtained the acceptable piezoelectric properties, which will make $BaTiO_3$ become a kind of promising and practical lead-free piezoelectric ceramics.

Keywords $BaTiO_3$·Li_2O · Low-temperature sintering · Piezoelectric properties

1 Introduction

Although lead-based piezoelectric ceramics such as Pb(Zr, Ti)O_3 (PZT) have been widely used as sensor, actuators, transformers as well as micro-electrical drivers due to their superior piezoelectric properties, the environmental concerns urgently call for lead-free materials to replace the PZT with high content of toxic lead [1]. Barium titanate ($BaTiO_3$) is one of the most promising candidates. Considerable efforts have been made to fabricate high performance $BaTiO_3$ lead-free piezoelectric ceramics by new methods. High piezoelectric constant d_{33} values of 350, 416, 460 and 788 pC/N were separately reported for those $BaTiO_3$ ceramics which were prepared by microwave sintering, spark plasma sintering, two-step sintering and templated grain growth using hydrothermally synthesized fine $BaTiO_3$ powders [2–5]. However, those unusual sintering techniques are unsuitable for mass production due to high cost or complex processes. It is essential to establish an economical production route to prepare $BaTiO_3$ ceramics with high piezoelectric properties.

The densification sintering temperature is about 1300°C for traditionally sintered $BaTiO_3$ ceramics. Its grains are easier to grow up at such a high sintering temperature, which is unfavorable to obtaining high-performance $BaTiO_3$ ceramics. It is commonly considered that much smaller grains should be required to obtain much higher piezoelectric properties [2, 4, 6]. In addition, it is difficult to co-fire $BaTiO_3$ and conductor interelectrodes such as low melting point Ag (961°C) or Ag/Pd alloys at high sintering temperatures, which restricts the applications of $BaTiO_3$ ceramics [7]. Lowering the sintering temperature becomes more significant to prepare high piezoelectric properties in the practical applications of $BaTiO_3$ ceramics. Sintering aids are mostly used to lower the sintering temperature of $BaTiO_3$ ceramics, among which Li^+-containing additives are very effective [8–10]. You [8] reported that the sintering temperature of (Ba,Sr)TiO_3 was reduced from 1350°C to 900°C by adding Li_2CO_3. Amin et al. [9] found that $BaTiO_3$ showed

N. Ma · B.-P. Zhang (✉) · W.-G. Yang
School of Materials Science and Engineering,
University of Science and Technology Beijing, China,
No.30 Xueyuan Road, Haidian Zone Beijing,
Beijing 100083, China
e-mail: bpzhang@ustb.edu.cn

an improved dielectric property after adding a minor LiF even that the sample was sintered below 900°C. An obvious reduction of the densification temperature from 1250°C to 900°C was also confirmed in the $Ba(Zr_xTi_{1-x})O_3$ system by adding Li_2O [10]. All of them made the densification temperature lower than the melting points of the conventional conductive materials like silver and gold. Both Li_2CO_3 and LiF have a low melting point, about 723°C and 846°C, respectively. Thereby they easily form liquid phase and promote the densification in the low temperature sintering. On the other hand, Li_2O, unlike Li_2CO_3 or LiF, has a high melting point above 1700°C, making it is impossible to form liquid phase directly in the low-temperature sintering process. So the detailed doping mechanism of Li_2O should be different from that of Li_2CO_3 or LiF. Valant [11] observed $BaCO_3$ from XRD pattern of the $BaTiO_3$-0.3wt%Li_2O sintered at 750°C for 5 h, suggesting that the sintering process involved an intermediate liquid phase $BaCO_3$ with a melting point of 811°C. Little attention was paid to studying the influence of Li_2O on piezoelectric properties of $BaTiO_3$ ceramics except for dielectric properties [11]. In the present study, low-temperature sintering of $BaTiO_3$-$x$$Li_2O$ (x=0–4 mol%) ceramics was investigated with special influences of Li_2O content and the sintering temperature on crystalline structure and electrical properties. A maximum d_{33} value (200 pC/N) was obtained for the $BaTiO_3$-0.5 mol%Li_2O sample even sintered at 1050°C.

2 Experimental

Barium titanate ($BaTiO_3$, 99 %) and lithium oxide (Li_2O, 98 %) were used as raw materials. These powders were weighed according to the chemical formula of $BaTiO_3$-$x$$Li_2O$ (x=0–4 mol%) and then mixed uniformly. The mixture was pressed into disks of 10 mm in diameter under 80 MPa using PVA as the binder, followed by normal sintering at 1000–1100°C for 2 h. Silver electrodes were fired at 600°C for 30 min on the top and bottom surfaces of the sintered samples. Poling was performed under an electric field of 3 kV/mm in silicone oil bath for 30 min.

Density of the sintered samples was determined by the Archimedes method. The crystal structure was determined using XRD with Cu $K\alpha$ radiation (λ=1.5416 Å) filtered through a Ni foil (Rigaku; RAD-B system, Tokyo, Japan). The microstructure of ceramic samples was observed by scanning electron microscope (SEM, ZEISS-EVO18, Germany) after chemically etching the sample surface in HCl:HF:H_2O=1:1:20 solution for 60 s. The piezoelectric constant d_{33} was measured using a quasi-static piezoelectric coefficient testing meter (ZJ-3A, Institute of Acoustics, Chinese Academy of Sciences, Beijing, China). The temperature dependence of dielectric properties was examined using a programmable furnace with an *LCR* analyzer (TH2828S) at 1 kHz between 11–200°C. Ferroelectric hysteresis loops were measured using a ferroelectric tester (RT6000HVA, Radiant Technologies, Inc., Albuquerque, NM).

3 Results and discussion

Figure 1 shows the XRD patterns of $BaTiO_3$-$x$$Li_2O$ ceramics sintered at 1050°C. It is apparent that the samples with x=0–3 mol% exhibit a pure perovskite structure. Further increasing x to 4.0 mol% gives rise to Ba_2TiO_4 (PDF#75-0677). The diffraction peaks cited from the tetragonal $BaTiO_3$ (PDF#05-0626) and the orthorhombic one (PDF#81-2200) are indicated by vertical lines for comparison. The enlarged XRD patterns of angle ranging from 38 ° to 40 ° are shown in Fig. 1(b). The tetragonal phase is characterized by a (111) peak and the orthorhombic phase splits (102)/(120) peaks at about 39 °. The (111) peak split into (102)/(120) peaks with increasing Li_2O content. The ratios of two diffraction peaks around 45 ° between PDF#05-0626 and PDF#81-2200 are obviously different as shown in the enlarged XRD patterns of angle ranging from 44 ° to 46 ° in Fig. 1 (c), in which the former ratio of (200) to (002) is greater than 1 but the later ratio of (200) to (022) is less than 1. All the diffraction peaks correspond well to those of the PDF#05-0626 for the samples x=0–0.3 mol% and the PDF#81-2200 for the counterparts x=0.5–4 mol%, respectively. This result suggests that the crystallographic structure changes from tetragonal symmetry to orthorhombic one with increasing x from 0.3 to 0.5 mol%. On the other hand, the diffraction peaks shift to lower angles by increasing x, which corresponds to the enlargement of the lattices owing to the substitution of Li^+ (0.76 Å) for Ti^{4+} (0.61 Å) [12, 13]. $BaTiO_3$-$x$$Li_2O$ ceramics sintered at 1000°C and 1100°C showed the similar XRD patterns to the samples sintered at 1050°C.

Figure 2 shows SEM images of chemically etched surface of $BaTiO_3$-$x$$Li_2O$ ceramics sintered at 1050°C. All the samples possess a uniform microstructure. Comparing Fig. 2(a) and 2(b), it is seen that adding a small amount of Li_2O (x=0.3 mol%) causes a slight grain growth, although the grain size is still less than 1 μm. The $BaTiO_3$-$x$$Li_2O$ (x=0–0.3 mol%) ceramics show a loose and porous structure. With increasing x to 0.5 mol% and 0.7 mol%, the grains grow suddenly to about 10 μm (Fig. 2(c)–2(d)). When x>1.0 mol%, the grains continually grow to about 20 μm (Fig. 2(e)–2(h)). It is commonly considered that liquid phase contributes to the grain growth in the low temperature sintering since the liquid phase facilitates the dissolution and migration of the species [7]. However, the high melting point (above 1700°C) of Li_2O makes it impossible to form directly

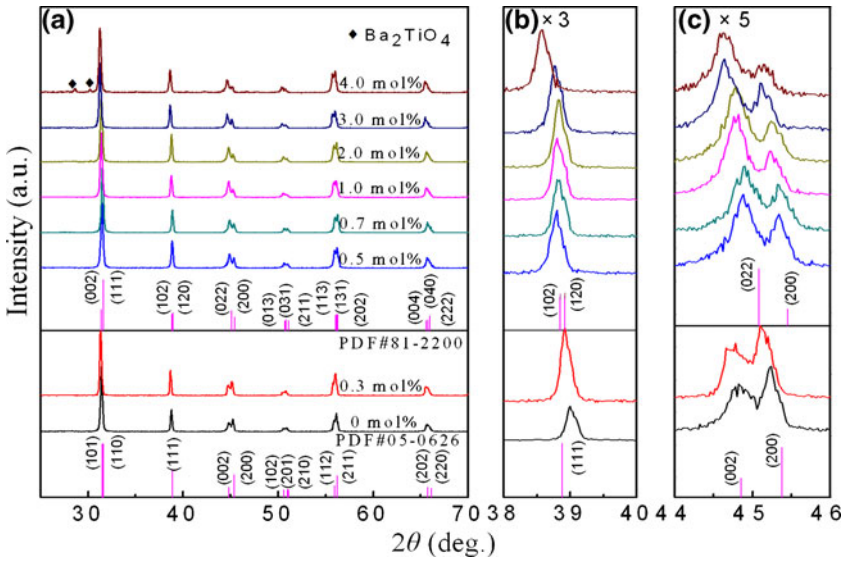

Fig. 1 XRD patterns of $BaTiO_3$-xLi_2O (0–4 mol%) ceramics sintered at 1050°C

liquid phase in the sintering process. Valant et al. [11] reported that $BaCO_3$ formed intermediately in the sintering process of Li_2O-doped $BaTiO_3$ ceramics based on a XRD pattern. The grain growth may be ascribed to the liquid phase sintering caused by the formation of $BaCO_3$ which has a low melting point (811°C). Apart from the liquid phase sintering mechanism, the emergence of oxygen vacancies may be another reason for the accelerated grain growth. The substitution of Li^+ ion for high valence Ti^{4+} leads to the creation of oxygen vacancies due to the ionic charge compensation, which is favorable to the mass transport during sintering and greatly promotes the grain growth [13].

Figure 3 delineates the variation of relative density ρ_r (a), piezoelectric constant d_{33} (b) dielectric constant ε_r (c) and dielectric loss tan δ (d) as functions of Li_2O content and the sintering temperature, respectively. The relative density of the pure $BaTiO_3$ is 71.2 %, 77.7 %, 85.4 % when the sintering was performed at 1000, 1050 and 1100°C, respectively, whereas a great enhancement of the relative density achieved by adding a small amount of Li_2O. The peak relative densities (90.5 %, 94.3 %, 95.0 %) shift toward reduced x (2.0, 0.7, 0.5 mol%) with the sintering temperature raising from 1000°C 1100°C. This fact indicates that the Li_2O promotes the sintering of $BaTiO_3$ which may be due to the intermediate liquid phase $BaCO_3$. When x exceeds the optimal value, the reduced relative density may be due to the formation of Ba_2TiO_4 with increasing x. The melting point of Ba_2TiO_4 is as high as 1860°C, which is harmful to the density in the liquid sintering process. Similar to the varying trend of the relative density with x, the d_{33} values of $BaTiO_3$-xLi_2O ceramics sintered at 1000, 1050 and 1100°C at first increase, peak at x=0.7, 0.5 and 0.5 mol%, respectively, and then turn to decrease with increasing x. It is worth noting that the optimal Li_2O content in the sample with the highest d_{33} was not fully consistent with the composition where the highest density was obtained. For example, the highest density is obtained at x=0.7 mol% for the sample sintered at 1050°C, but the d_{33} value shows a maximum (200 pC/N) at x=0.5 mol% and decreases to 185 pC/N at x=0.7 mol%. The result can be understood because the piezoelectric properties depend not only on density but also on grain sizes and phase transition. The samples of x=0.5 mol% and x=0.7 mol% possess a compact structure and similar grain sizes, so the grain sizes may be not the main factor to influence the d_{33}. On the other hand, the sample with x=0.5 mol% is closer to the phase transition between tetragonal phase and orthorhombic one, which provides a favorable condition for easier motion of domain and thus gives rise to the higher piezoelectric properties. The peak d_{33} value at x=0.5 mol% should be attributed to the dual effects of the high relative density and the phase transition. The crystallographic structure transition of $BaTiO_3$-xLi_2O has a great influence on the piezoelectric properties, which is similar to those of the $(Na,K)NbO_3$-based ceramics [14–16]. Likewise, the highest relative density and the maximum d_{33} values are obtained for the samples sintered at 1000°C at x=2.0 mol% and x= 0.7 mol%, respectively. The substitution of high valence Ti^{4+} ions for Li^+ will lead to the creation of more oxygen vacancies for ionic charge compensation, which pins the movement of the ferroelectric domain walls. The pinning of domain walls is much stronger with increasing x, and results in a decrease of d_{33}. The ε_r of pure $BaTiO_3$ shows the maximum value at the room temperature, then it reduces with increasing Li_2O content. It is well known that the ε_r of perovskite materials are generally correlated with phase structure, grain sizes, and defect species [17]. Adding Li_2O evoked the transition from tetragonal to orthorhombic phase and promoted the grain growth, which associated with oxygen vacancies may further deteriorate the dielectric

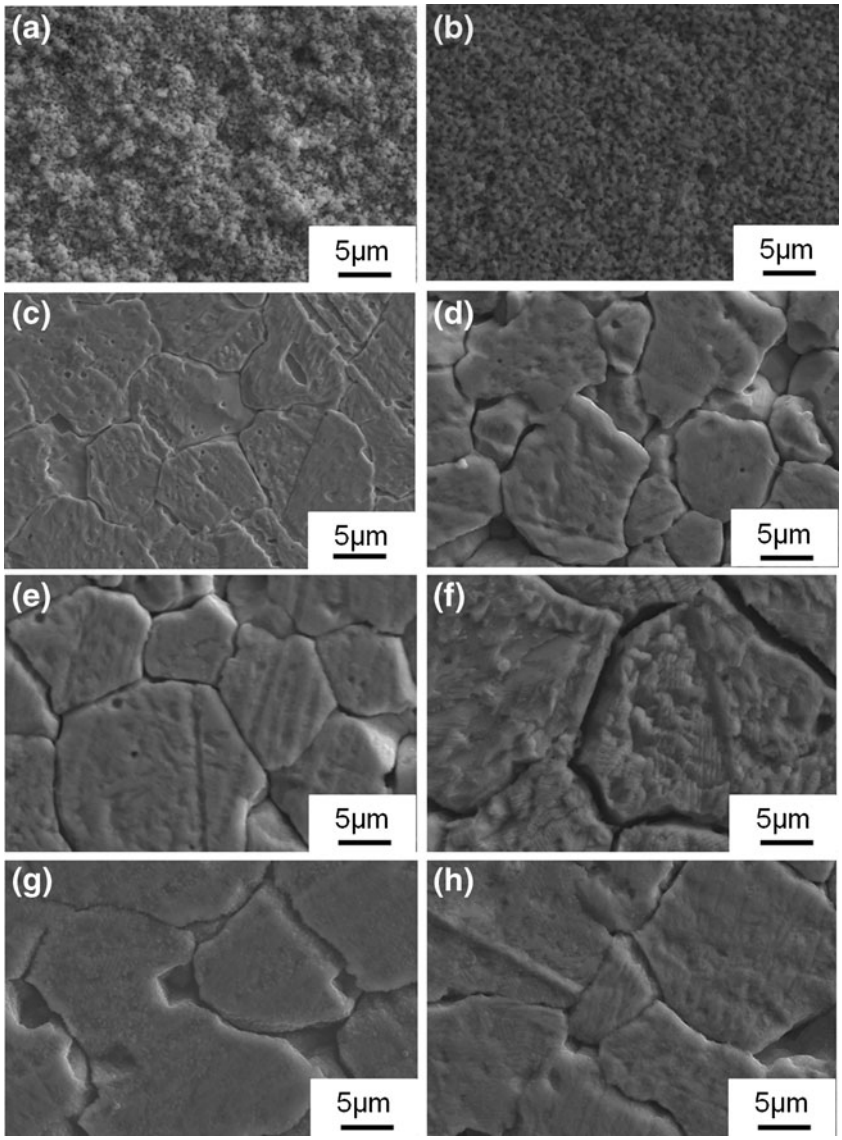

Fig. 2 SEM images of $BaTiO_3$-xLi_2O (0–4 mol%) ceramics sintered at 1050°C for 2 h. (**a**) x=0, (**b**) x=0.3, (**c**) x=0.5, (**d**) x=0.7, (**e**) x=1.0, (**f**) x=2.0, (**g**) x=3.0, (**h**) x=4.0 mol%

properties. The tan δ of $BaTiO_3$-xLi_2O ceramics increase at the beginning and then decrease with increasing x.

The properties of recently reported $BaTiO_3$-based ceramics are summarized in Table 1. All the ceramic samples were fabricated by a conventional solid-state reaction method except the $Ba_{0.9}K_{0.1}TiO_{2.9}F_{0.1}$ ceramic which was prepared by spark plasma sintering (SPS). Sintering aids greatly lowered the sintering temperature of $BaTiO_3$-based ceramics. In this study, the sintering temperature for $BaTiO_3$-0.05 mol%Li_2O is reduced by 160°C as compared with that (1210°C) of pure $BaTiO_3$. Meanwhile, their piezoelectric properties are comparable with those of other $BaTiO_3$-based ceramics. The Tc of $BaTiO_3$-0.05 mol%Li_2O is kept at 120°C and no decreasing trend was found by adding Li_2O.

Figure 4 shows the temperature dependence (11–200°C) of dielectric constant ε_r for the $BaTiO_3$-xLi_2O ceramics measured at 1 kHz. The T_C of the pure $BaTiO_3$ is 120°C, and it increases to 125°C when Li_2O content is above 0.7 mol%. The inset in Fig. 4 shows the temperature dependence of dielectric constant ε_r at 11–25°C. A dielectric constant peak exists in the range of 11–25°C, which corresponds to the orthorhombic–tetragonal phase transition temperature ($T_{O\text{-}T}$). The $T_{O\text{-}T}$ is 17, 22, 23, 23, 24°C for samples with x=0, 0.5, 0.7, 2.0, 4.0, respectively, which shows a slightly increased trend of $T_{O\text{-}T}$ with increasing Li_2O content. Why the current $T_{O\text{-}T}$ is higher than that ($T_{O\text{-}T}$~5°C) reported commonly for $BaTiO_3$ ceramics [3] is still unknown. A similar $T_{O\text{-}T}$ (19°C) for $BaTiO_3$ ceramics sintered at 1210°C was also found based on a DSC experimental without any explanation [3]. Nevertheless, the increased trend of $T_{O\text{-}T}$ with increasing Li_2O content is consistent with the phase transition in XRD patterns (Fig. 1). The sample of x=0.5 mol% is close to the orthorhombic–tetragonal transition at the room temperature as shown in Fig. 1, which contributes to the excellent piezoelectric properties.

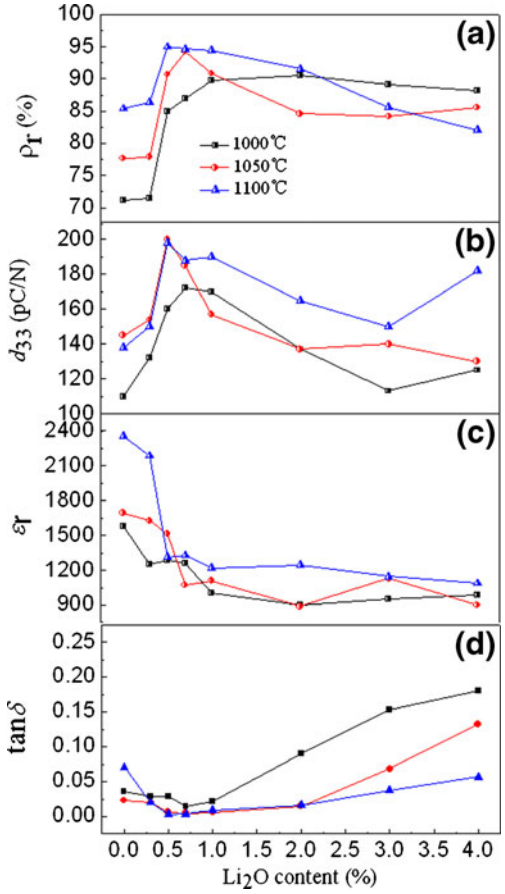

Fig. 3 Relative density (**a**), piezoelectric constant (**b**), dielectric constant (**c**) and dielectric loss (**d**) of $BaTiO_3$-xLi_2O (0–4 mol%) ceramics sintered at 1000–1100°C

Figure 5 shows the ferroelectric hysteresis loops of $BaTiO_3$-xLi_2O ceramics sintered at 1050°C and pure $BaTiO_3$ sintered at 1200°C. Comparing with the pure $BaTiO_3$ sintered at 1200°C whose relative density was 95.2 % [20], the pure $BaTiO_3$ sintered at 1050°C shows an unsaturated hysteresis loop with low relative density (77.7 %). Besides the density, the microstructure and crystallographic structure may be the other factors to affect the shape of hysteresis loop. The pure $BaTiO_3$ sintered at 1200°C possesses much denser microstructure comparing with the sample sintered at 1050°C. The $BaTiO_3$ samples sintered at 1050°C and 1200°C were tetragonal symmetry and

Table 1 The properties of recently reported $BaTiO_3$-based ceramics

Ceramic system	d_{33}(pC/N)	Sintering temperature (°C)	T_c(°C)	ε_r	Refs.
$BaTiO_3$	419	1210	–	3181	[6]
$Ba(Zr_{0.05}Ti_{0.95})O_3$-1.5wt%$Li_2O$	120	900	107	1250	[10]
$BaTiO_3$-4 mol% LiF	270	1100	65	3500	[18]
$Ba_{0.9}K_{0.1}TiO_{2.9}F_{0.1}$(SPS)	230	1000	47	–	[19]
$BaTiO_3$-0.05 mol%Li_2O	200	1050	120	1977	This work

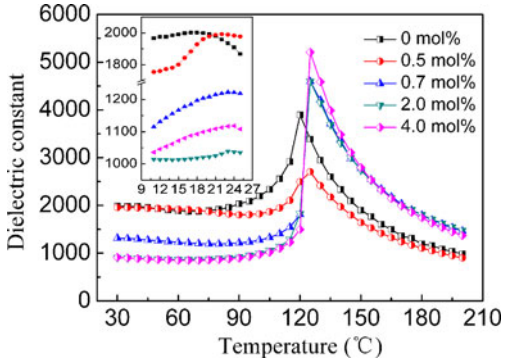

Fig. 4 Temperature dependence of the dielectric constant at 1 kHz for $BaTiO_3$-xLi_2O (0–4 mol%) ceramics sintered at 1050°C

orthorhombic one, respectively. The later one was closer to the phase transition between tetragonal symmetry and orthorhombic one [20], which provides a favorable condition for easier motion of domain and gives rise to the increase of the P_r. Therefore, the pure $BaTiO_3$ sintered at 1200°C showed a saturated hysteresis loop. Although the sample with x=0.05 mol% has a high relative density of 94.4 %, the hysteresis loop is not as saturated as the pure $BaTiO_3$ sample sintered at 1200°C, which may be due to the increased oxygen vacancies. The oxygen vacancies are created by adding Li_2O, which is harmful to the P_r. Both relative density and oxygen vacancies greatly affect the shape of hysteresis loop. The polarization hysteresis loops become thinner with increasing Li_2O content. When the Li_2O content reaches 0.7 mol%, a double loop is gradually observed. The defect dipoles are formed by the acceptor dopant ions Li^+ and oxygen vacancies along the spontaneous polarization direction. Because of the low migration rates of defects, the defect dipoles remain in the original orientation, providing a restoring force to reverse the switched polarization, thus giving a small P_r [21]. The inset in Fig. 5 illustrates the variation of the remanent polarization P_r and E_c of $BaTiO_3$-xLi_2O. The P_r at first increases and then decreases. The sample x=0.5 mol% shows a maximum P_r value of 2.0

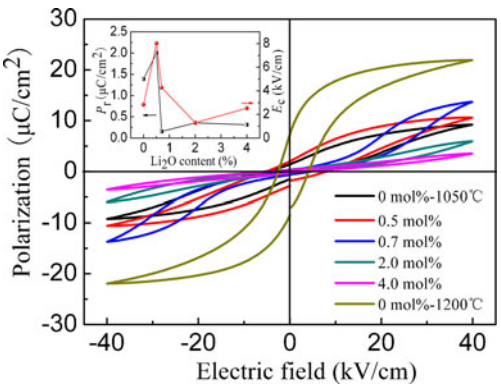

Fig. 5 Ferroelectric hysteresis loops of the $BaTiO_3$-xLi_2O (0–4 mol%) ceramics sintered at 1050°C and pure $BaTiO_3$ sintered at 1200°C

μC/cm^2, with a corresponding E_c value of 8.0 kV/cm. However, more oxygen vacancies are created for ionic charge compensation with increasing Li_2O content, which strengthen the pinning effect to the ferroelectric domain under an electric field, thereby inducing a continuous decline of the P_r [13]. How to reduce the oxygen vacancies to obtain excellent ferroelectricity for $BaTiO_3$-xLi_2O ceramics requires further investigation.

4 Conclusions

The influences of Li_2O content and sintering temperature on the phase structure, density, and electrical properties of the $BaTiO_3$- xLi_2O (x=0–4 mol%) ceramics were investigated. The crystallographic structure of $BaTiO_3$-xLi_2O ceramics changes from tetragonal phase to orthorhombic one with increasing x. Adding Li_2O accelerates the grain growth because of the liquid phase sintering caused by the low melting point of $BaCO_3$. The densification sintering temperature is 1000°C, which is about 300°C lower than that of pure $BaTiO_3$ sample. $BaTiO_3$ ceramic with x=0.05 mol% sintered at 1050°C exhibits d_{33}=200 pC/N, ε_r=1977, P_r=2.0 μC/cm^2, because it is near the phase transition between tetragonal symmetry and orthorhombic one in addition to its high density.

Acknowledgments This work was supported by Specialized Research Fund for the Doctoral Program of Higher Education (Grant No. 20090006110010) and Beijing Natural Science Foundation (Grant No.2112028)

References

1. P.K. Panda, J. Mater. Sci. **44**, 5049 (2009)
2. H. Takahashi, Y. Numamoto, J.J. Tani, S. Tsurekawa, Jpn. J. Appl. Phys. **45**, 7405 (2006)
3. Z.Y. Shen, J.F. Li, J. Ceram. Soc. Jpn. **118**, 940 (2010)
4. K. Karaki, K. Yan, M. Adachi, Jpn. J. Appl. Phys. **46**, 7035 (2007)
5. S. Wada, K. Takeda, T. Muraishi, H. Kakemoto, T. Tsurumi, T. Kimura, Jpn. J. Appl. Phys. **46**, 7039 (2007)
6. S.F. Shao, J.L. Zhang, Z. Zhang, P. Zheng, M.L. Zhao, J.C. Li, C.L. Wang, J. Phys. D: Appl. Phys. **41**, 125408 (2008)
7. Y.D. Hou, L.M. Chang, M.K. Zhu, X.M. Song, H. Yan, J. Appl. Phys. **102**, 084507 (2007)
8. H.W. You, J.H. Koh, Integr. Ferroelectr. **93**, 46 (2007)
9. D. Prakash, B.P. Sharma, T.R. Rama Mohan, P. Gopalan, J. Solid State Chem. **155**, 86 (2000)
10. N. Binhayeeniyi, P. Sukvisut, C. Thanachayanont, S. Muensit, Mater. Lett. **64**, 305 (2010)
11. M. Valant, D. Suvorov, R.C. Pullar, J. Eur. Ceram. Soc. **26**, 2777 (2006)
12. L. Taïbi-Benziada, H.S. Hilal, R. Mühll, Solid State Sci. **8**, 922 (2006)
13. N. Lei, M.K. Zhu, P. Yang, L.L. Wang, L.F. Wang, Y.D. Hou, H. Yan, J. Appl. Phys. **109**, 054102 (2001)
14. P. Zhao, R. Tu, T. Goto, B.P. Zhang, S. Yang, J. Am. Ceram. Soc. **91**, 3440 (2008)
15. H.T. Li, B.P. Zhang, P.P. Shang, Y. Fan, Q. Zhang, J. Am. Ceram. Soc. **94**, 628 (2011)
16. K. Wang, J.F. Li, N. Liu, Appl. Phys. Lett. **93**, 092904 (2008)
17. A. Singh, K. Sreenivas, R.S. Katiyar, V. Gupta, J. Appl. Phys. **102**, 074110 (2007)
18. W.G. Yang, B.P. Zhang, N. Ma, L. Zhao, J. Eur. Ceram. Soc. **32**, 899 (2011)
19. Y. Akishige, Y. Hiraki, S. Tsukada, J. Xu, S. Morito, T. Ohba, E.L. Walker, A. Neogi, Jpn. J. Appl. Phys. **49**, 081501 (2010)
20. N. Ma, B.P. Zhang, W.G. Yang, D Guo. J. Eur. Ceram. Soc. **32**, 1059 (2011)
21. D. Lin, K.W. Kwok, H.L.W. Chan, Appl. Phys. Lett. **90**, 232903 (2007)